



The influence of the thioalkyl terminal group on the mesomorphic behavior of some 6-alkoxy-2-naphthoates derived from 1,3,4-oxadiazole

N. J. Chothani, V. K. Akbari, P. S. Patel & K. C. Patel

To cite this article: N. J. Chothani, V. K. Akbari, P. S. Patel & K. C. Patel (2016) The influence of the thioalkyl terminal group on the mesomorphic behavior of some 6-alkoxy-2-naphthoates derived from 1,3,4-oxadiazole, *Molecular Crystals and Liquid Crystals*, 631:1, 31-46, DOI: [10.1080/15421406.2016.1147329](https://doi.org/10.1080/15421406.2016.1147329)

To link to this article: <http://dx.doi.org/10.1080/15421406.2016.1147329>



Published online: 12 Jul 2016.



Submit your article to this journal [↗](#)



Article views: 52



View related articles [↗](#)



View Crossmark data [↗](#)

The influence of the thioalkyl terminal group on the mesomorphic behavior of some 6-alkoxy-2-naphthoates derived from 1,3,4-oxadiazole

N. J. Chothani^a, V. K. Akbari^b, P. S. Patel^c, and K. C. Patel^b

^aArts, Science and Commerce College, Kholwad, Surat, Gujarat, India; ^bDepartment of Chemistry, Veer Narmad South Gujarat University, Surat, Gujarat, India; ^cDepartment of Chemistry, Narmada College of Science and Commerce, Zareshwar, Bharuch, India

ABSTRACT



A new series of mesogenic compounds having a naphthalene moiety has been synthesized by esterification of 4-(5-(alkylthio)-1,3,4-oxadiazol-2-yl)phenol and 6-alkoxy-2-naphthoic acid and their liquid crystalline properties have been studied. All the members of the series are enantiotropic and exhibit smectic as well as nematic mesophase. The plot of transition temperatures versus number of carbon atoms in the alkoxy chain exhibits no odd even effect and falling tendency for isotropic transition temperatures. High anisotropy, linearity confers rich mesomorphic properties on the system.

KEYWORDS

Calamitic liquid crystal; nematic N phase; smectic A phase; smectic C phase; thioalkyl

1. Introduction

Liquid crystal (LC) science is one the most important topic in current years, even though to establish correlation between chemical structure and mesomorphic properties in important problems. It is an important and challenging task for the chemists to synthesize mesomorphic organic compounds with required physical-chemical characteristics and allows understanding of the influence of different structural elements of the molecule architecture. The thermotropic mesomorphism of calamitic LC is largely influenced by molecular structure in which a slight change brings about considerable change in its properties [1,2]. It is well established that the linearity is prime and foremost criteria for the rod-like calamitic LC's molecular geometry, which is generally achieved by using aromatic, heteroaromatic, or aliphatic rings as mesogenic units. On the other hand, some functional central bridging groups have proven to be very useful to promote mesomorphic properties. During the last decades, heterocycles are considerably used in the molecular architectures of novel organic materials, especially in the development of thermotropic LCs. Mesomorphic compounds containing heterocyclic units have been synthesized and interest has dramatically increased due to their diversified molecular structure and distinct mesomorphic properties [3–12]. The incorporation of heterocyclic moieties for the design of new mesogenic molecules can result in large changes in their mesophases and physical properties. In addition, introduction of heteroatoms can cause

CONTACT K. C. Patel  drkcpatel55@gmail.com  Department of Chemistry, Veer Narmad South Gujarat University, Surat–395 007, Gujarat, India.

Color versions of one or more of the figures in the article can be found online at www.tandfonline.com/gmcl.

© 2016 Taylor & Francis Group, LLC

considerable changes in polarity, polarizability, and geometry of the molecules because most of the heteroatoms (S, O, and N) are more polarizable than carbon. These factors lead to dramatic changes in the corresponding mesophase type, the phase transition temperatures [13,63]. Heterocycle cores are thus able to impart lateral and/or longitudinal dipoles combined with changes in the molecular shape [14,15]. Dipole-dipole interactions and structural shapes are fundamental elements in the design of LCs [16]. Among these derivatives, the five-membered heterocyclic rings, such as 1,3,4-oxadiazoles, have also proven to be highly efficient in promoting mesomorphic properties [17–22]. The introduction of oxadiazole rings not only provide lateral dipole from the oxygen and nitrogen atoms, but also the bent shape of the rigid cores. This large lateral dipole leads to the increase possibility may leads to very interesting mesomorphic properties, when oxadiazole rings are used as central cores [23].

In recent years, mesogenic 1,3,4-oxadiazole derivatives have been extensively investigated, by many research group [24–42]. Recently, Han has also been reported a review on 1,3,4-oxadiazole derivatives, in which a great attention has been paid on the structure-property relationship [43]. Since this type of compound may exhibit tunable liquid crystalline properties with fluorescence with high quantum yields, together with excellent thermal and chemical stability and they have strong electron affinity and often possess electron transport properties [44–47]. Compounds involving the 1,3,4-oxadiazole ring have been used as emitter in organic electroluminescent devices [48–50] and also be used as a mesogenic core to construct organic light-emitting diodes among the heterocyclic compounds [51,52]. The materials containing the 1,3,4-oxadiazole unit hold great potential for use to synthesize different fluorescent chemosensors for transition metal ions [53], biologically active agents [54], and scintillators [55].

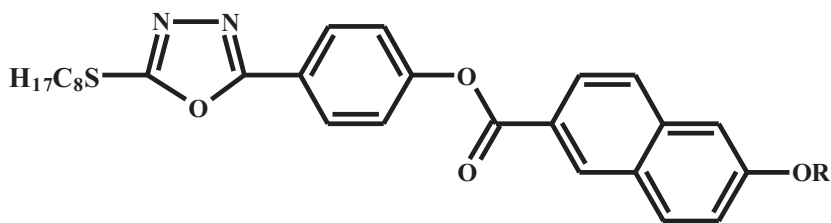
In 1989, Chudgar *et al.* first reported a series of liquid crystalline 1,3,4 oxadiazoles, which exhibited nematic phase with high melting points [56]. Mahadeva *et al.* synthesized another homologous series of 2-amino-5-alkoxyphenyl-1,3,4-oxadiazoles, which showed relatively lower melting points [57]. Parra group [58,59] synthesized a series of 1,3,4-oxadiazole derivatives and the effect of the 1,3,4-oxadiazole moiety on liquid crystalline properties was investigated systematically. In investigations of liquid crystalline esters of 2,5-bis-(4-hydroxyphenyl)-1,3,4-oxadiazoles and 2-alkylthio-5-(4-hydroxyphenyl)-1,3,4-oxadiazoles, it was established that the esters of 2-alkylthio-5-(4-hydroxyphenyl)-1,3,4-oxadiazoles showed the widest mesomorphic ranges and these compounds exhibited smectic A (SmA) and nematic (N) phases [60].

The main aim of this work is to obtain calamitic LCs with different phases and to study the effect of length of the thioalkyl chain and the effect of the heterocyclic moiety (1,3,4-oxadiazoles) on the mesomorphic properties. To the best of our knowledge, there are reports on the 2-alkylthio-5-(4-hydroxyphenyl)-1,3,4-oxadiazoles which are interesting systems for the design and synthesis of liquid crystalline compounds with a classical rod-like structure. The introduction of a 1,3,4-oxadiazole ring within core of calamitic molecules strongly influences their mesomorphic behavior due (though not only) to the dipolar moment associated with the heterocyclic ring.

Experimental

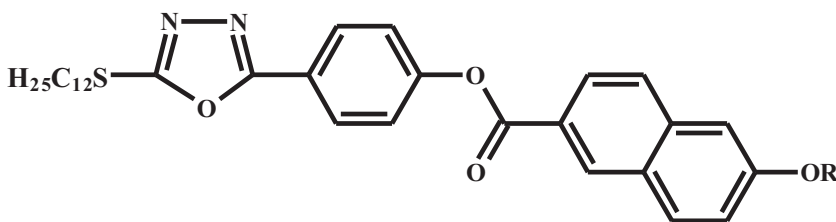
Methods and materials

For the synthesis of compounds of the homologous series, following materials were used. 4-Hydroxybenzoic acid was purchased from Spectrochem, alkyl bromide (Lancaster),



4-(5-(octylthio)-1,3,4-oxadiazol-2-yl)phenyl-6-alkoxy-2-naphthoate

Series I



4-(5-(dodecylthio)-1,3,4-oxadiazol-2-yl)phenyl-6-alkoxy-2-naphthoate

Series II

Where, $R = C_nH_{2n+1}$, $n = 1$ to 8, 10, 12, 14, 16

4-(dimethylamino)pyridine (DMAP), and N,N' -dicyclohexylcarbodiimide (DCC) were purchased from Aldrich. The solvents were used after purification using the standard methods described in the literature.

Elemental analysis (C, H, and N) were performed on Thermo Finnigan EA 1112 Flash Elemental Analyzer. Fourier transform infrared spectra were recorded with Shimadzu DRS 8400-S Spectrophotometer (Shimadzu IR Solution 1.30 software) in the frequency range 4000–400 cm^{-1} with samples embedded in KBr discs. ^1H NMR (300 MHz) and ^{13}C NMR (75 MHz) spectra of the compound were recorded with BRUKER AVANCE II Spectrometer (Bruker BioSpin AG, Fallanden, Switzerland; 300 MHz) using CDCl_3 as a solvent and TMS as an internal reference. Mass spectra (EI) of the compounds were recorded with Advion Expression CMS, USA (Compact Mass Spectrometer) using ESI as ionization source. Thin-layer plates (Merck 60 F524) are examined under short-wave UV light. The product was purified by column chromatography over silica gel (60–120 mesh, Sigma-Aldrich Co.). UV-visible spectra were recorded with Thermo Scientific Evolution 300 UV-VIS. Thermal analyses, differential scanning calorimetry (DSC) of the liquid crystalline compounds were performed on Perkin Elmer, Model: DSC7 Series using Pyris Software, heating rate of $10^\circ\text{C}/\text{min}$ in N_2 atmosphere. The thermobalance and temperature calibration (with Pt-100) was checked by standard sample. The optical microscopy studies were carried out with NICON ECLIPSE 50i POL (Japan) with hot stage and the temperature controller Linkam Analyssa-LTS420. The textures of the compounds were observed using polarized light with crossed with sample in thin film sandwiched between a glass slide and cover slip.

Synthesis

Synthesis of 6-Alkoxy-2-naphthoic Acid (2)

6-Hydroxy-2-naphthoic acid (**1**) (2.44 g, 13 mmol, 1 equiv.) and KOH (1.46 g, 26 mmol, 2 equiv.) were dissolved in ethanol/water (25 mL, 9/1) and the solution was stirred for 20 min; corresponding *n*-alkyl bromide (32.50 mmol, 2.5 equiv.) was then added and the mixture is heated under reflux for 24 hr. When the reaction was complete, KOH (0.73 g, 13 mmol, 1 equiv.) was added and the mixture is heated under reflux for further 4 hr. The ethanol was evaporated, and the mixture is poured into water and acidified to approximately pH = 2~3 with acetic acid. The precipitate was filtered and washed with water and ether, and then recrystallized twice from glacial acetic acid, then from ethanol to give 71%~80% yield. (IR) (KBr): $\nu_{\text{max}}/\text{cm}^{-1}$: 3061, 2930, 2828, 1680, 1603, 1311, 1472, 1450, 1383, 1216, 1060, and 721.

Synthesis of Ethyl 4-hydroxybenzoate (4)

A solution of 4-hydroxybenzoic acid (**3**) (25 g, 181 mmol), ethanol (30 mL) were mixed, then H_2SO_4 was added (catalytic amount), resultant mixture was heated at 80–85°C for 3 hr. After the completion of the reaction, concentrated and solid residue was poured in 400 mL of ice-cooled water. The solid was removed by filtration, wash with water, and dried. The crude solid was twice recrystallized from ethanol (yield: 90%).

Synthesis of 4-Hydroxybenzohydrazide (5)

A solution of methyl ethyl 4-hydroxybenzoate (**4**) (14.9 g, 90 mmol) and excess of a solution of hydrazine hydrate (80%) in 20 mL of ethanol was heated to reflux during 8 hr. The mixture was then cooled to room temperature and the solid obtained was filtered, washed with water, and recrystallized from ethanol (yield: 87%).

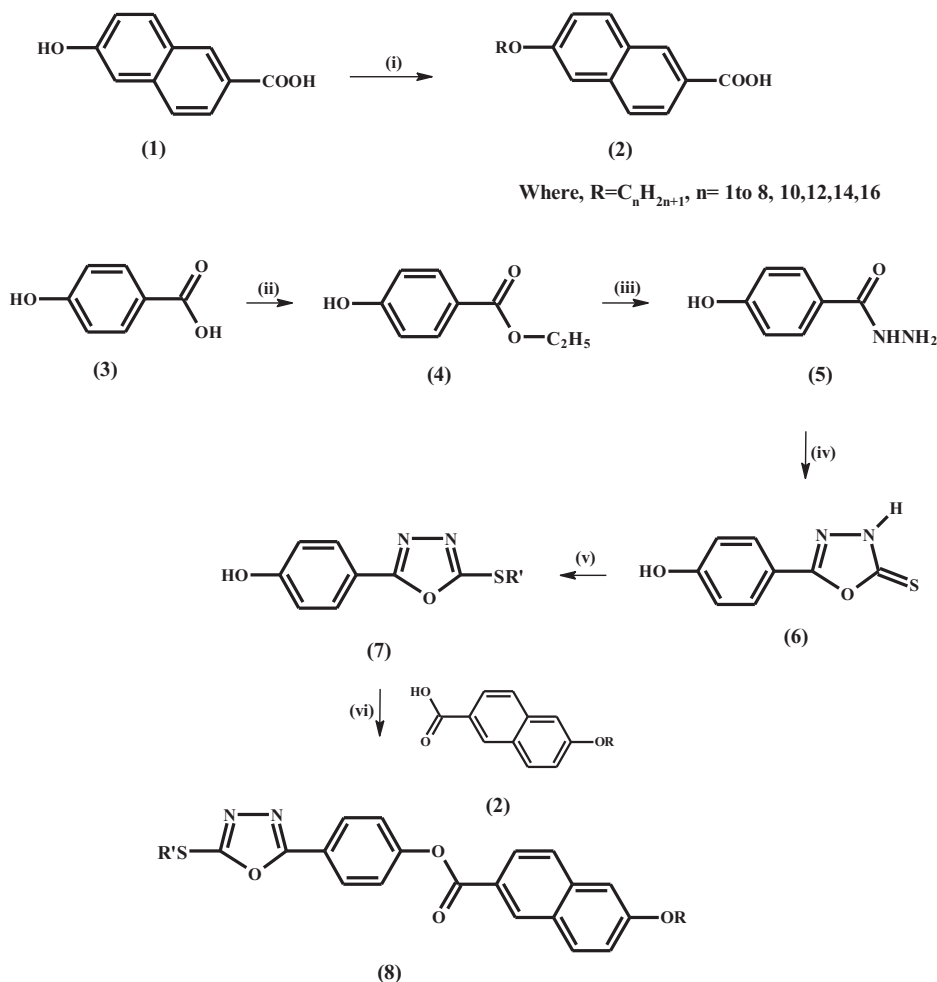
Synthesis of 5-(4-Hydroxyphenyl)-1,3,4-oxadiazole-2(3H)-thione (6)

A suspension of 4-hydroxybenzohydrazide (**5**) (8.5 g, 56 mmol, 1 equiv.) in ethanol (20 mL) was stirred, then a solution of KOH (3.13 g, 56 mmol, 1 equiv.) in water (20 mL) was added dropwise to this stirred suspension at 25°C. After all of the hydrazide has dissolved, carbon disulphide (4.2 mL, 70 mmol, 1.25 equiv.) was added at the same temperature and stirring was continuing for 2 hr. After the completion of the reaction, solution was evaporated and crude was poured into a mixture of 300 g ice-cooled water, then the solution was carefully acidify with concentrated hydrochloric acid. The light brown solid formed was filtered off and recrystallized from water:ethanol (1:9) (yield: 67%) [59].

Synthesis of 4-(5-(Alkylthio)-1,3,4-oxadiazol-2-yl)phenol (7)

A solution of 5-(4-hydroxyphenyl)-1,3,4-oxadiazole-2(3H)-thione (**6**) (7 g, 36 mmol, 1 equiv.) in absolute ethanol (50 mL) was stirred, to this solution triethylamine (5 mL, 36 mmol, 1 equiv.) and corresponding *n*-alkylbromide (36 mmol, 1 equiv.) were successively added dropwise. Then, reaction mixture was reflux for 6 hr, after completion of the reaction solvent was

evaporated. The residue was poured into 300 mL of water, the resulting precipitate was collected. The compound was purified by column chromatography over silica gel (60–120 mesh), using 7%–8% dichloromethane:methanol as eluent (yield:92%) [59] (Scheme 1).



Where, $R = C_nH_{2n+1}$, $n = 1 \text{ to } 8, 10, 12, 14, 16$

Where, $R' = C_8H_{17}$ (Series I)
 $= C_{12}H_{25}$ (Series II)

Scheme 1. Reagents and Reaction conditions: (i) R-Br, KOH, ethanol, reflux 28 hr, (ii) ethanol, H_2SO_4 , (iii) NH_2NH_2 (80%), (iv) CS_2 , KOH, (v) Et_3N , RBr, and (vi) DCC, DMAP, dry CH_2Cl_2 , stirring 24 hr.

Synthesis of 4-(5-(Alkylthio)-1,3,4-oxadiazol-2-yl)phenyl-6-alkoxy-2-naphthoate (Series I and II)

A compound 4-(5-(alkylthio)-1,3,4-oxadiazol-2-yl)phenol (7) (1.8 mmol, 1 equiv.), corresponding 6-alkoxy-2-naphthoic acid (1.8 mmol, 1 equiv.) and DMAP (0.008 g, 0.08 mmol, 0.05 equiv.) were stirred in anhydrous CH_2Cl_2 (10 mL). To this solution, DCC (0.56 g,

2.7 mmol, 1.5 equiv.) in CH_2Cl_2 (2 mL) added slowly at room temperature and the mixture was stirred for 24 hr at room temperature. After the completion of the reaction, the white solid N,N' -dicyclohexylure was filtered off; the filtrate was diluted with CH_2Cl_2 (20 mL), then was washed thoroughly with 4% HCl, saturated NaHCO_3 and twice with water. The organic layer was separated, dried over Na_2SO_4 , and evaporated. The product was purified by column chromatography over silica gel (60–120 mesh), using 40% hexane:ethyl acetate as eluent and recrystallized from the solvent mixture dichloromethane:ethanol (1:9) obtain slight brown solid (yield: 83–91%) [61–63].

Compound I₇: Yield: 89%; transitions ($^{\circ}\text{C}$): Cr 131 N 170 Iso; UV-Vis (CHCl_3) λ_{max} (nm): 260, 293; ^1H NMR (CDCl_3): δ (ppm) = 0.87–0.90 (t, J = 7.6 Hz, 6H, 2CH_3), 1.25–1.89 (m, 22H, 11CH_2), 3.23–3.28 (t, J = 6.1 Hz, 2H, SCH_2), 4.06–4.11 (t, J = 6.2 Hz, 2H, OCH_2), 7.19 (d, J = 8.2 Hz, 2H, Ar-H), 7.31 (dd, J = 2.2, 9.0 Hz, 1H, naphthalene), 7.57 (dd, J = 1.8, 8.5 Hz, 1H, naphthalene), 7.86 (d, J = 1.6 Hz, 1H, naphthalene), 7.92 (d, J = 8.4 Hz, 1H, naphthalene), 8.01 (d, J = 8.8 Hz, 1H, naphthalene), 8.10 (s, 1H, naphthalene), and 8.14 (d, J = 8.8 Hz, 2H, Ar-H); ^{13}C NMR (CDCl_3): δ (ppm) = 14.12 (CH_3 aliphatic), 22.62–32.60 (CH_2 aliphatic), 32.71 (SCH_2), 68.26 (OCH_2), 106.47–159.63 (aromatic C), 164.78, 165.20 (oxadizole ring), and 165.79 ($\text{C}=\text{O}$); IR (KBr) ν_{max} (cm^{-1}): 3030, 3064 (C–H str. aromatic), 2921, 2851 (C–H str. aliphatic), 1735 ($\text{C}=\text{O}$ str. ester), 1627 ($\text{C}=\text{N}$ str. oxadizole), 1575, 1534 ($\text{C}=\text{C}$ str. aromatic), 1278 (C–O str. ester), 1218 (C–O–C asym. str. alkoxy), and 1067 (C–O–C sym. str. alkoxy); MS m/z (rel. int.%): 575.3 ($\text{M}+1$)⁺; elemental analysis for $\text{C}_{34}\text{H}_{42}\text{N}_2\text{O}_4\text{S}$: Calc.: C=71.05%, H = 7.37%, and N = 4.87%; Found: C=70.86%, H = 7.32%, and N = 4.97%.

Compound I₁₆: Yield: 91%; transitions ($^{\circ}\text{C}$): Cr 64 smectic C (SmC) 88 SmA 155 Iso; UV-Vis (CHCl_3) λ_{max} (nm): 261, 293; ^1H NMR (CDCl_3): δ (ppm) = 0.85–0.87 (t, J = 7.6 Hz, 6H, 2CH_3), 1.25–1.89 (m, 40H, 20CH_2), 3.23–3.28 (t, J = 6.2 Hz, 2H, SCH_2), 4.07–4.011 (t, J = 6.2 Hz, 2H, OCH_2), 7.06–8.15 (m, 10H, aromatic H), 7.12 (d, J = 8.1 Hz, 2H, Ar-H), 7.30 (dd, J = 1.8, 9.0 Hz, 1H, naphthalene), 7.55 (dd, J = 2.1, 8.7 Hz, 1H, naphthalene), 7.80 (d, J = 1.8 Hz, 1H, naphthalene), 7.88 (d, J = 8.4 Hz, 1H, naphthalene), 7.92 (d, J = 8.8 Hz, 1H, naphthalene), 8.09 (s, 1H, naphthalene), and 8.11 (d, J = 8.7 Hz, 2H, Ar-H); ^{13}C NMR (CDCl_3): δ (ppm) = 14.12 (CH_3 aliphatic), 22.69–32.57 (CH_2 aliphatic), 32.69 (SCH_2), 68.29 (OCH_2), 106.43–163.58 (aromatic C), 164.85, 165.13 (oxadizole ring), and 165.82 ($\text{C}=\text{O}$); IR (KBr) ν_{max} (cm^{-1}): 3034, 3064, 3119 (C–H str. aromatic), 2929, 2852 (C–H str. aliphatic), 1734 ($\text{C}=\text{O}$ str. ester), 1627 ($\text{C}=\text{N}$ str. oxadizole), 1574, 1523 ($\text{C}=\text{C}$ str. aromatic), 1272 (C–O str. ester), 1215 (C–O–C asym. str. alkoxy), and 1064 (C–O–C sym. str. alkoxy); MS m/z (rel. int. %): 701.2 ($\text{M}+1$)⁺; elemental analysis for $\text{C}_{43}\text{H}_{60}\text{N}_2\text{O}_4\text{S}$: Calc.: C=73.67%, H = 8.63%, and N = 4.00%; Found: C=73.60%, H = 8.47%, and N = 3.97%.

Compound II₇: Yield: 89%; transitions ($^{\circ}\text{C}$): Cr 110 SmA 159 Iso; UV-Vis (CHCl_3) λ_{max} (nm): 261, 291; ^1H NMR (CDCl_3): δ (ppm) = 0.87–0.90 (t, J = 7.4 Hz, 6H, 2CH_3), 1.25–1.89 (m, 30H, 15CH_2), 3.23–3.28 (t, J = 6.3 Hz, 2H, SCH_2), 4.09–4.13 (t, J = 6.1 Hz, 2H, OCH_2), 7.12 (d, J = 8.5 Hz, 2H, Ar-H), 7.40 (dd, J = 1.9, 8.8 Hz, 1H, naphthalene), 7.55 (dd, J = 1.8, 8.7 Hz, 1H, naphthalene), 7.80 (d, J = 1.5 Hz, 1H, naphthalene), 7.87 (d, J = 8.4 Hz, 1H, naphthalene), 7.96 (d, J = 8.8 Hz, 1H, naphthalene), 8.12 (s, 1H, naphthalene), and 8.14 (d, J = 8.6 Hz, 2H, Ar-H); ^{13}C NMR (CDCl_3): δ (ppm) = 14.12 (CH_3 aliphatic), 22.62–32.21 (CH_2 aliphatic), 32.79 (SCH_2), 68.27 (OCH_2), 106.49–159.64 (aromatic C), 164.78, 165.20 (oxadizole ring), and 165.80 ($\text{C}=\text{O}$); IR (KBr) ν_{max} (cm^{-1}): 3034, 3060, 3120 (C–H str. aromatic), 2923, 2851 (C–H str. aliphatic), 1733 ($\text{C}=\text{O}$ str. ester), 1627 ($\text{C}=\text{N}$ str. oxadizole), 1574, 1535 ($\text{C}=\text{C}$ str. aromatic), 1283 (C–O str. ester), 1217 (C–O–C asym. str. alkoxy), and 1066 (C–O–C sym. str. alkoxy); MS m/z (rel. int.%): 631.4 ($\text{M}+1$)⁺; elemental analysis for

$C_{38}H_{50}N_2O_4S$: Calc.: C=72.35%, H = 7.99%, and N = 4.44%; Found: C=72.26%, H = 7.87%, and N = 4.38%.

Compound II₁₆: Yield: 91%; transitions (°C): Cr 68 SmC 82 SmA 146 Iso; UV-Vis ($CHCl_3$) λ_{max} (nm): 261, 291; 1H NMR ($CDCl_3$): δ (ppm) = 0.85–0.89 (t, J = 7.2 Hz, 6H, $2CH_3$), 1.25–1.89 (m, 48H, $24CH_2$), 3.24–3.28 (t, J = 6.2 Hz, 2H, SCH_2), 4.11–4.13 (t, J = 6.3 Hz, 2H, OCH_2), 7.21 (d, J = 8.5 Hz, 2H, Ar-H), 7.32 (dd, J = 2.1, 9.0 Hz, 1H, naphthalene), 7.68 (dd, J = 1.7, 8.4 Hz, 1H, naphthalene), 7.80 (d, J = 1.8 Hz, 1H, naphthalene), 7.88 (d, J = 8.2 Hz, 1H, naphthalene), 7.92 (d, J = 8.8 Hz, 1H, naphthalene), 8.05 (s, 1H, naphthalene), and 8.19 (d, J = 9.0 Hz, 2H, Ar-H); ^{13}C NMR ($CDCl_3$): δ (ppm) = 14.12 (CH_3 aliphatic), 22.69–32.21 (CH_2 aliphatic), 32.80 (SCH_2), 68.28 (OCH_2), 106.50–159.65 (aromatic C), 163.86, 165.22 (oxadizole ring), and 165.82 ($C=O$); IR (KBr) ν_{max} (cm^{-1}): 3035, 3061, 3119 (C–H str. aromatic), 2920, 2850 (C–H str. aliphatic), 1734 ($C=O$ str. ester), 1626 ($C=N$ str. oxadizole), 1573, 1536 ($C=C$ str. aromatic), 1284 (C–O str. ester), 1220 (C–O–C asym. str. alkoxy), and 1066 (C–O–C sym. str. alkoxy); MS m/z (rel. int.%): 757.2 ($M+1$)⁺; elemental analysis for $C_{47}H_{68}N_2O_4S$: Calc.: C=74.56%, H = 9.05%, and N = 3.70%; Found: C=74.49%, H = 9.09%, and N = 3.68%.

Result and discussion

In this article, we report the synthesis and phase characterization of a homologous series of 1,3,4-oxadiazole achiral asymmetrical four-ring calamitic liquid crystalline compounds, as a feature of their structure-property relationships. The molecular structures of these newly synthesized compounds were characterized by spectroscopic methods. The thermotropic liquid crystalline behavior of the achiral rod-like 1,3,4-oxadiazole compounds, series I and II, was studied using polarizing optical microscopy (POM) and DSC.

Thermal and phase behavior

Mesomorphic properties of series I and II were determined by DSC and POM. The phase transition temperatures, reported in this article, were the peak values of the transition on the DSC curves. Phase identification was made by comparing the observed textures with those reported in the literature. The phase transition temperatures, the associate enthalpy changes, and the mesophase textures of the series I and II are summarized in Tables 1 and 2, respectively. Clearcut transition temperatures and textures were obtained from the DSC and POM

Table 1. Transition temperature data of the series I.

Compounds	$R = n$ alkoxy	Transition temperature (°C)							
		Cr	SmC	SmA	N	I			
I ₁	Methyl	•	—	—	—	151	•	193	•
I ₂	Ethyl	•	—	—	—	146	•	188	•
I ₃	Propyl	•	—	—	—	140	•	184	•
I ₄	Butyl	•	—	—	—	139	•	179	•
I ₅	Pentyl	•	—	—	—	136	•	177	•
I ₆	Hexyl	•	—	—	—	134	•	172	•
I ₇	Heptyl	•	—	—	—	131	•	170	•
I ₈	Octyl	•	77	•	99	•	—	169	•
I ₁₀	Decyl	•	72	•	95	•	—	165	•
I ₁₂	Dodecyl	•	69	•	93	•	—	161	•
I ₁₄	Tetradecyl	•	66	•	89	•	—	158	•
I ₁₆	Hexadecyl	•	64	•	88	•	—	155	•

Table 2. Transition temperature data of the series II.

Compounds	<i>R</i> = <i>n</i> alkoxy	Transition temperature (°C)								
		Cr	SmC		SmA		N*		I	
II ₁	Methyl	•	—	—	—	—	152	•	183	•
II ₂	Ethyl	•	—	—	—	—	149	•	176	•
II ₃	Propyl	•	—	—	—	—	144	•	169	•
II ₄	Butyl	•	—	—	—	—	141	•	168	•
II ₅	Pentyl	•	—	—	—	—	136	•	164	•
II ₆	Hexyl	•	—	—	116	•	131	•	161	•
II ₇	Heptyl	•	—	—	110	•	—	—	159	•
II ₈	Octyl	•	87	•	106	•	—	—	153	•
II ₁₀	Decyl	•	83	•	104	•	—	—	151	•
II ₁₂	Dodecyl	•	79	•	96	•	—	—	150	•
II ₁₄	Tetradecyl	•	73	•	89	•	—	—	147	•
II ₁₆	Hexadecyl	•	68	•	82	•	—	—	146	•

observations for the representative compounds, and were in good agreement with each other for heating cycles.

All the compounds synthesized in series I are mesomorphic in nature. The smectic mesophase commences from the *n*-octyloxy derivative. *n*-Octyloxy to *n*-hexadecyloxy (C₈, C₁₀, C₁₂, C₁₄, and C₁₆) members exhibit an enantiotropic SmC coexist with SmA phase. Transition temperature shows that compounds I₁ to I₇ displayed enantiotropic nematic phase, while no smectic phase was observed. After sufficient length increment, smectic mesophase is exhibit in case of higher homologous. It is well known that the stability of the mesophase would be augmented by an increase in the polarity or polarizability of the mesogenic part of the molecule. The relative strength of the lateral and terminal cohesive forces between molecules determines the type of the mesophase formed [64]. The thermal stability of a smectic mesophase is largely determined by the low ratio of terminal to lateral intermolecular cohesive forces while a high ratio of these forces is important in determining nematic mesophase. Since the dipolar (alkoxy) and polarizable (ester) centers of the molecule have become further separated from one another as a result of the lengthened alkyl chain, the terminal intermolecular attraction has decreased while the residual lateral attractions are essentially unchanged. This increases the ratio of lateral to terminal cohesive forces, makes the probability greater that the layer arrangement, which is characteristic of the smectic mesophase, will persist after melting occurs. Changes in this ratio are, therefore, quite important in determining the type of the mesomorphism being exhibited by certain molecule in a series of liquid crystalline compounds as well as the temperature at which mesomorphic transition occur [65]. Strong lateral and weak terminal intermolecular cohesions will give rise to a smectic mesophase, which, if the lateral cohesions are high enough, may persist until the isotropic liquid is formed [64]. Therefore, in series I higher homologues exhibit only enantiotropic smectic mesophase. This is because the long chains become attracted and intertwined, which facilitates the lamellar packing required for smectic phase generation. As a result, the smectic tendency increases and eventually eliminates the nematic phase. A plot of transition temperatures against the number of carbon atoms in the alkoxy chain given in Fig. 1. It shows a steady fall in the temperature of smectic, nematic, and isotropic transitions.

Similarly, all the 12 members of series II exhibit either enantiotropic nematic or smectic mesophase. The SmA and SmC phases commence from the *n*-hexyloxy and *n*-octyloxy derivative, respectively, as enantiotropic mesophase and remain up to the *n*-hexadecyloxy derivative. In series II, C₁ to C₆ members show enantiotropic nematic phase, among them C₆ member also coexist with SmA phase. The melting clearing temperatures of

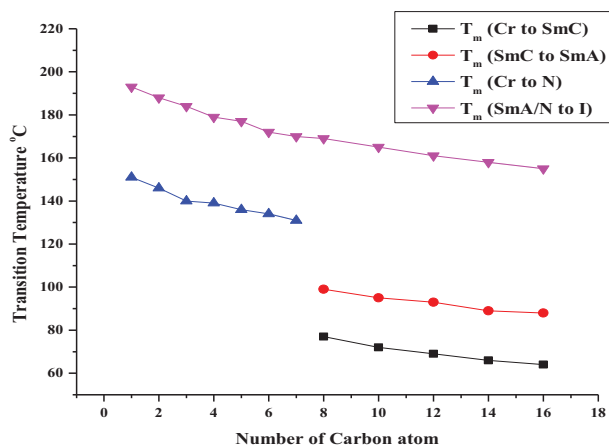


Figure 1. Transition temperature curve for series I.

series II are recorded in Table 2 and a plot of transition temperatures against the number of carbon atoms in the alkoxy chain given in Fig. 2.

It can be noticed that mesophase transition temperatures decrease with the increase in the length of terminal alkoxy tail. The plot of transition temperature against the number of carbon atom in the alkoxy chain shows a smooth falling tendency for mesomorphic-isotropic transition temperature throughout the series. Series II exhibits falling tendency of T_{Cr-N} and T_{Cr-SmA} and exhibits falling tendency of $T_{SmC-SmA}$ transition temperatures for higher homologous.

DSC is a valuable method for the detection of phase transitions. It yields quantitative results; therefore, we may draw conclusions concerning the nature of the phases that occur during the transition. In the present study, DSC measured enthalpy of two derivatives of series I and II. DSC data of series I and II are recorded in Table 3, which further help to confirm the mesophase. Table 3 shows the phase transition temperatures, associated enthalpy (ΔH), and molar entropy (ΔS) for compounds of series I (I_7 and I_{16}), series II (II_7 and II_{16}). The DSC curves of representative compounds of the series I and II are shown in Figs. 3(a,b) and 4(a,b). Microscopic transition temperature values are almost similar to DSC data.

Table 4 shows average thermal stabilities and mesophase range of compounds of series I and II. The T_{N-I} thermal stabilities of compounds of series I and II are 180.42°C and 168.57°C

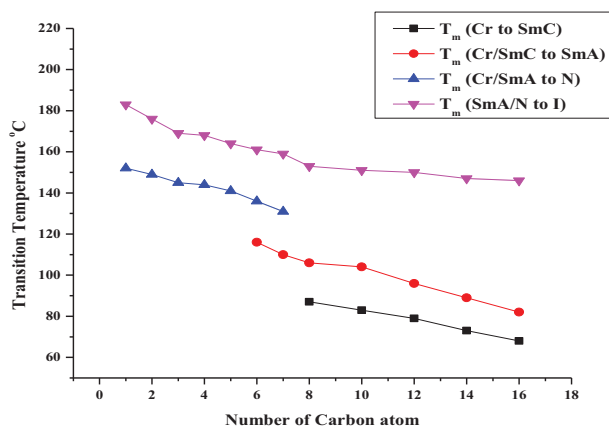


Figure 2. Transition temperature curve for series II.

Table 3. Transition temperature and DSC data of the series I and II.

Compound	Transition	Microscopic temp. (peak temp.) (°C)	ΔH (J g ⁻¹)	ΔS (J g ⁻¹ k ⁻¹)
I ₇	Cr-N	127.95(131)	82.642	0.2061
	N-I	166.36(170)	2.006	0.0045
I ₁₆	Cr-SmC	65.35(64)	77.883	0.2301
	SmC-SmA	84.33(88)	2.856	0.0079
	SmA-I	152.42(155)	3.306	0.0077
II ₇	Cr-SmA	108.10(110)	61.092	0.1603
	SmA-N	124.32(131)	2.516	0.0063
	N-I	157.00(159)	3.219	0.0074
II ₁₆	Cr-SmC	72.42(68)	56.229	0.1627
	SmC-SmA	79.83(82)	3.421	0.0096
	SmA-I	150.79(146)	4.140	0.0097

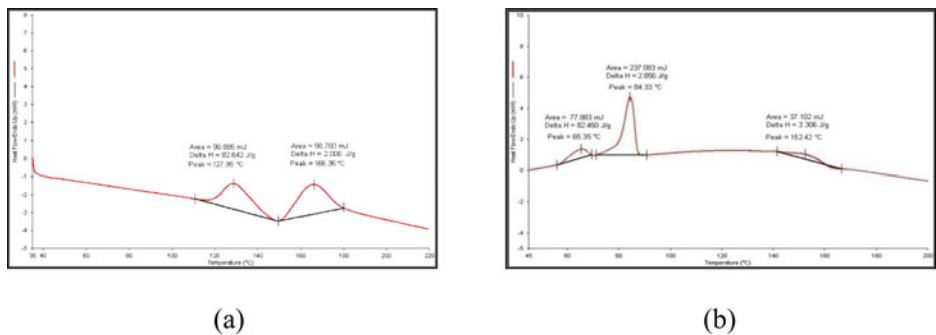


Figure 3. (a) DSC thermogram of compound I₇ (series I) and (b) DSC thermogram for compound I₁₆ (series I).

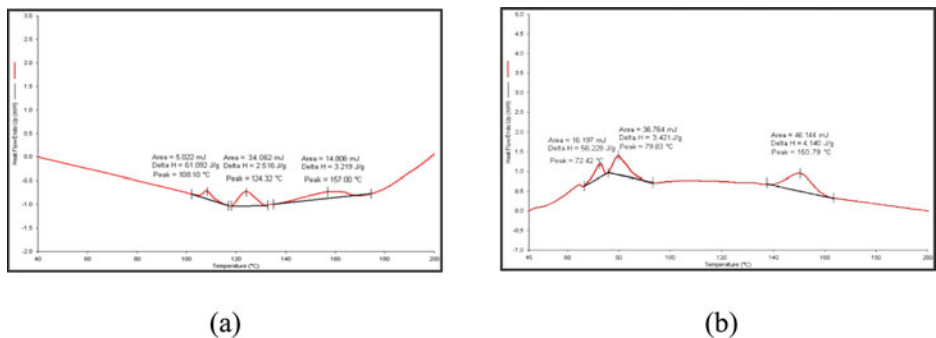


Figure 4. (a) DSC thermogram of compound II₇ (series II) and (b) DSC thermogram for compound II₁₆ (series II).

Table 4. Average thermal and mesophase stabilities of the series I and II.

Series	I	II	Diff.
N-I (°C)	180.42	168.57	11.85
SmA-I (°C)	161.60	149.40	12.20
SmA-N (°C)	—	133.50	—
SmC-SmA (°C)	90.8	95.4	4.60
N mesophase range (°C)	29.71	19.14	10.87
SmC mesophase range (°C)	19.0	13.6	5.40
SmA mesophase range (°C)	28.6	31.14	2.54
Commencement of smectic phase	C ₈	C ₆	—

and $T_{\text{SmA-I}}$ thermal stabilities are 161.60°C and 149.40°C, respectively. The $T_{\text{SmC-SmA}}$ thermal stabilities of compounds of series I and II are 90.8°C and 95.4°C, respectively. Series II also shows $T_{\text{SmA-N}}$ thermal stability about 133.5°C. From the Table 4, it can be seen that the average SmC mesophase range of compounds of series I and II are 19.0°C and 13.6°C and average SmA mesophase range are 28.6°C and 31.14°C, respectively. The average nematic mesophase range of compounds of series I and II are 29.71°C and 19.14°C, respectively.

Structure-mesomorphic property relationships

Intermolecular interactions are extremely important in understanding the mesogenic behavior of LCs. The melting point (the temperature at which an ordered geometrical arrangement collapses and gives rise to the ordered isotropic melt) depends largely on the nature of the intermolecular interaction existing within the system. The cycle of mesomorphism (heating or cooling) and the transition temperature are governed by the intermolecular forces that act between the planes and ends of the molecule. It is generally agreed that the prime requirement for the formation of a thermotropic LC is anisotropy in the molecular interaction [64].

In this article, at one end thioalkyl group is fixed, i.e., series I having $-\text{SC}_8\text{H}_{17}$, series II having $-\text{SC}_{12}\text{H}_{25}$, and alkoxy chain length of 6-alkoxy-2-naphtioic acid is varied. It has been observed that compounds of series I have higher transition temperature than that of the compounds of series II. This may be attributed to the shorter alkoxy chain giving higher temperature than the longer alkoxy chain. For compounds with longer terminal chains, of series II, cooling the nematic phase resulted in an additional SmA phase is appeared from C_6 member, while C_8 member in case of series I. The dependence of the transition temperatures on the total chain length can be seen by comparing series I and II in which the two terminal chains are of the different length. While both the melting and clearing temperatures fall with increasing chain length, the reduction of the clearing temperatures is more significant. For the shortest chain, compound of series I, the widest mesophase range, was seen from Table 1. Increasing the chain length decreases the temperature range of the compounds of series II, with decyloxy chains. Further symmetry lowering, by introducing two chains of different lengths as appears in series I and II to stabilize the mesophase range. Compounds of series II have a longer total chain length by an extra methylene units than compounds of series I, therefore, its transition temperatures are expected to be lower and its mesophase range should be smaller. Interestingly, compounds of series II not only showed a higher SmA mesophase range but also lower melting and clearing points. The most pronounced difference between these two series is the nematic phase range. The unequal chain lengths do not appear to disrupt the lamellar structure; indeed, a much wider smectic range is found for series I and II.

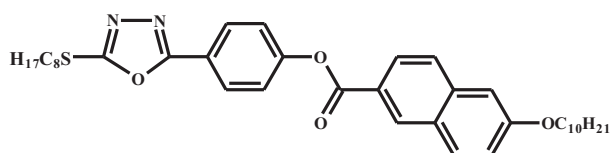
As shown in Table 4 differences in thermal stability as well as mesophase range of the compounds of series I and II. The overall thermal stability of compounds of series I is higher than that of compounds of series II. The nematic-isotropic transition is higher in compounds of series I by 11.85°C than compounds of series II. The compounds of series II have SmC-SmA thermal stabilities higher by 4.6°C than those of compounds of series I. The thermal stabilities of SmA phase of compounds of series I is also higher by 12.20°C than that of compounds of series II. The SmC mesophase average width of compound of series I is higher by 5.4°C than that of series II, while comparing the SmA mesophase range of compounds of series I is lower by 2.54°C than that of compounds of series II. The nematic mesophase width of compounds of series I is higher by 10.87°C than that of compounds of series II. However, the addition of a methylene group increases the overall polarizability of the molecule

[64]. Consequently, the lateral intermolecular attractions increase, as the chain length grows. Each methylene unit force apart polarizable centers in the molecule and decrease the residual terminal attraction. There should be a relative decrease in the strength of the terminal intermolecular cohesive interactions [64]. This will decreased the nematic-isotropic transition temperature. So, in series II having lower nematic-isotropic transition temperature than in series-I. In series I terminal intermolecular cohesive interactions is more due to shorter alkoxy chain at one terminal compare to series II.

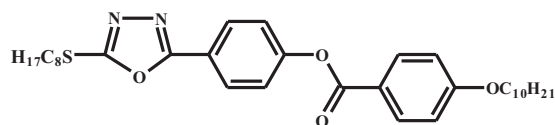
The influence on the thermal behavior of replacing one of the naphthyl units in compounds I_{10} and II_{10} , with a phenyl unit (compounds 2.5 and 2.9), is shown in the Table 5. Table 5 summarizes the transition temperature of the present compounds I_{10} and II_{10} and the structurally related compounds 2.5 and 2.9. In compound I_{10} , SmC phase is observed at 72°C, whereas in compound 2.5 it is observed at 75°C. The SmA mesophase is appeared form 95°C in compound 2.5, while it is observed at 95°C in compound I_{10} . The compound II_{10} shows SmC

Table 5. The Comparison of Transition Temperatures (°C) of representative Compound K_{10} and L_{10} of the present Series I & II and structurally related Compound 2.5 and 2.9

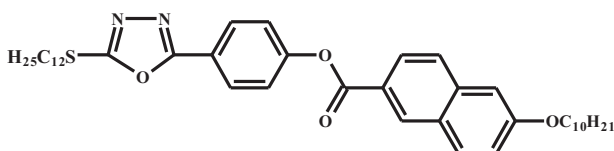
Compound	Transition temperature °C					
	Cr		SmC		SmA	N
I_{10}	•	72	•	95	•	-
II_{10}	•	83	•	104	•	-
2.5	•	75	•	95	-	•
2.9	•	85	•	116	•	-



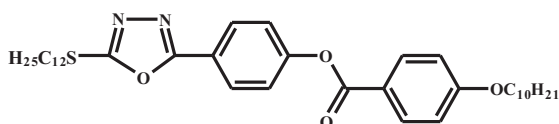
Compound I_{10}



Compound 2.5



Compound II_{10}



Compound 2.9

Scheme 2. Comparison of existing I_{10} and II_{10} compounds with structurally related compound 2.5 & 2.9. As shown in Table 5.

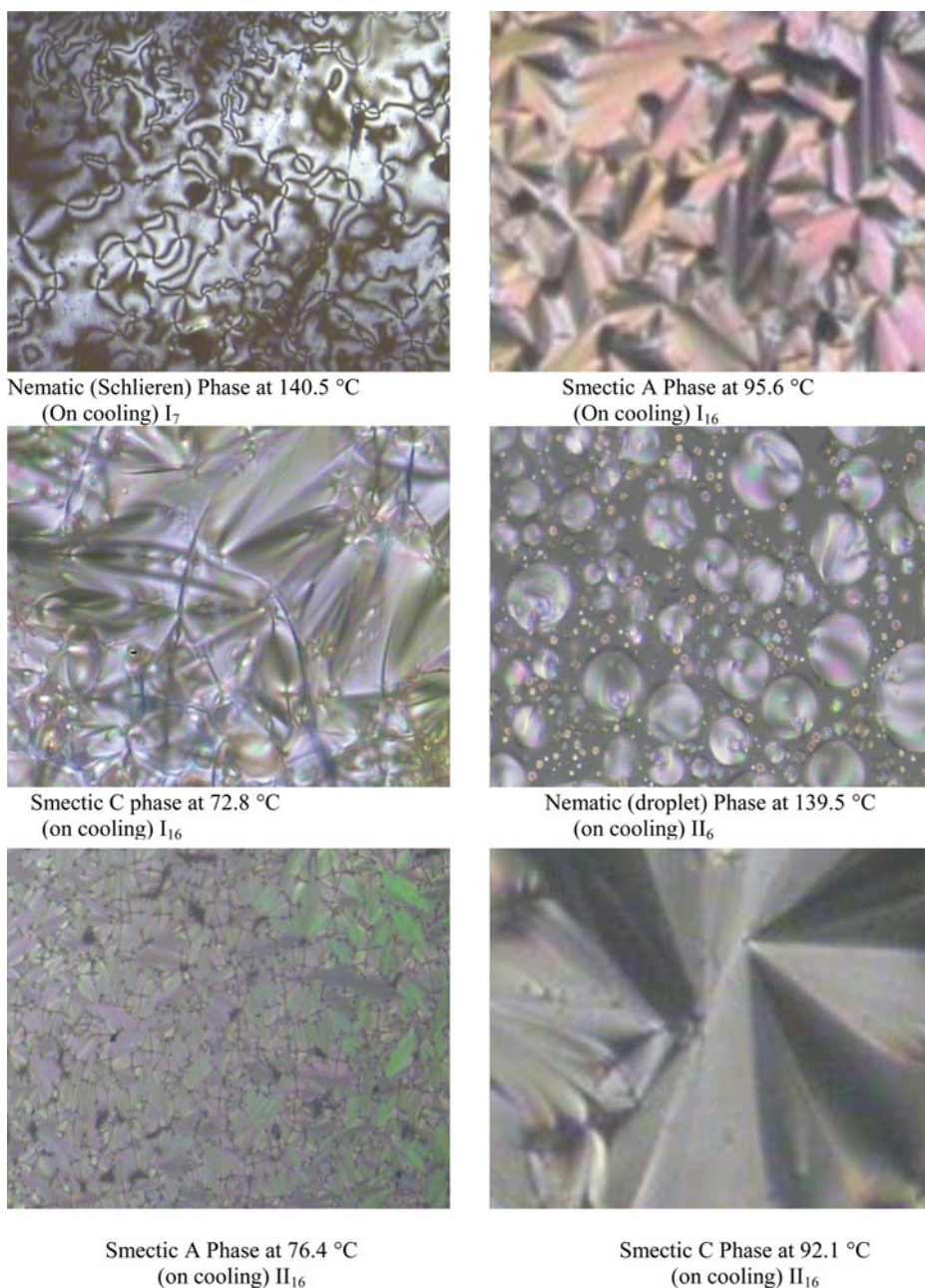


Figure 5. Microphotograph of liquid crystalline compounds.

phase at 83°C and SmA phase at 104°C, that is, 85°C and 116°C for compound 2.9. The clearing point temperature of both compounds I₁₀ and II₁₀ are higher than that of compounds 2.5 and 2.9. This due the fact that upper transition points for 6-*n*-alkoxy-2-naphthoic acids are higher than those for *p*-*n*-alkoxybenzoic acids with the same alkyl groups, by an average of 47°C, therefore, 6-*n*-alkoxy-2-naphthoic acids are more mesomorphic. Thus, despite their smaller molecular breadths (6.8 Å) the benzoic acids are less mesomorphic than the naphthoic acids (7.9 Å). Moreover, the molecules of the naphthoic acids are longer by 2.2 Å, but unlike the increases in a homologous series, this greater length results from the presence of

the second aromatic ring of the naphthalene nucleus. This will contribute more to the intermolecular cohesion than a single benzene ring and so enhances the thermal stability. Due to above reason, the compounds I₁₀ and II₁₀ have higher smectic thermal stability compare with its benzene analogue compounds 2.5 and 2.9.

Texture study

The optical microscopy studies were carried out with a “NICON ECLIPSE 50i POL” (Japan) equipped with LinkamAnalyse-LTS 420 hot stage. The textures of the compounds were observed using polarized light with crossed polarizers with sample in thin film sandwiched between a glass slide and cover slip. The textures of compounds of series I and II are shown in Fig. 5. Compound I₇ shows nematic phase on cooling the isotropic at 140.5°C. The nematic phase was confirmed by the appearance of a planar Schlieren texture or a homeotropic dark texture observed under polarized light microscopy. Compound II₁₆ shows focal conic fan-like texture of SmA phase on cooling the isotropic liquid at 95.6°C, on further cooling the SmA phase displayed broken fan-shape texture of SmC phase at 72.8°C. Compound II₆ shows droplet nematic phase on cooling the isotropic at 139.5°C. Compound II₁₆ shows simple fan-like texture of SmA phase on cooling the isotropic at 76.4°C and also displayed characteristic broken fan-like texture of SmC phase at 92.1°C.

Conclusion

We have synthesized and studied the thermal behavior of an altogether new set of rod-like molecules, in which the mesogenic (6-alkoxy-2-naphthoic acid) core is combined covalently with the 1,3,4-oxadiazole segment through a ester linkage. The length of thioalkyl chain, as well as the length of the alkoxy tail were varied to understand the structure-property correlation. It is clear that the length of the alkoxy chain had an influence, not only on the nature of the mesophases but also on the mesomorphic temperature ranges. Tables 1 and 2 illustrate the transition temperatures of compounds of series I and II during heating, as a function of the number of methylenic units (*n*) in the alkoxy chain. In general, an increase in terminal length resulted in enhanced dipole-dipole interaction between the terminal chains, leading to stability of the mesophases in rod-like mesogens. The length of thioalkyl chain is varied in both series. With lower length of thioalkyl chain, in series I, shows not only higher clearing point with wider mesophase range, with longer the thioalkyl chain shows lower in clearing point, but also having much considerable mesophase range. However, the presence of nitrogen, sulfur, or oxygen atoms in these heterocyclic rings [59], which probably introduce a transverse dipole moment, often, result in a change in dielectric anisotropy. The formation of liquid crystallinity in such heterocyclic compounds might be facilitated by weak π - π interaction between these aromatic or heterocyclic rings.

References

- [1] Dierking, I. (2006). *Textures of Liquid Crystals*, Chapter 1, Wiley-VCH: Weinheim, Germany.
- [2] Bodern, N., & Movaghar B. (1998). In: *Handbook of Liquid Crystals*, Demus, D., Goodby, J. W., Gray, G. W., Spiess, H. W., & Vill, V. (Eds.), Wiley-VCH: Chichester, U.K.
- [3] Seed, A. (2007). *Chem. Soc. Rev.*, 36, 2046.
- [4] Polshettiwar, V., & Varma, R. (2008). *Tetrahedron Lett.*, 49, 879.

- [5] Gallardo, H., Conte, G., Tuzimoto, P. A., Behramand, B., Molin, F., Eccher, J. A., & Bechtold, I. H. (2012). *Liq. Cryst.*, 39, 1099.
- [6] Tsai, H. H. G., Chou, L. C., Lin, S. C., Sheu, H. S., & Lai, C. K. (2009). *Tetrahedron Lett.*, 50, 1906.
- [7] Sato, M., Ohta, R., Hand, M., & Kasuga, K. (2002). *Liq. Cryst.*, 29, 1441.
- [8] Karamysheva, L. A., Torgova, S. I., & Agafonova, I. F. (2000). *Liq. Cryst.*, 27, 393.
- [9] Zhang, L., Chen, X., Zhao, F., Fan, X., Chen, P., & An, Z. (2013). *Liq. Cryst.*, 40, 396.
- [10] Benbayer, C., Saidi-Besbes, S., Grelet, E., & Derdour, A. (2013). *Liq. Cryst.*, 40, 1520.
- [11] (a) Ghosh, S., Begum, N., Turlapati, S., Kr. Roy, S., Kr. Das, A., & Rao, N. V. S. (2014). *J. Mater. Chem. C*, 2, 425; (b) Getmanenko, Y. A., Kang, S. W., Shaky, N., Pokhrel, C., Bunge, S. D., Kumar, S., Ellmanb, B. D., & Twieg, R. J. (2014). *J. Mater. Chem. C*, 2, 256; (c) Getmanenko, Y. A., Kang, S. W., Shaky, N., Pokhrel, C., Bunge, S. D., Kumar, S., Ellmanb, B. D., & Twieg, R. J. (2014). *J. Mater. Chem. C*, 2, 2600.
- [12] Elgueta, E. Y., Parra, M. L., Diaz, E. W., & Barbera, J. (2014). *Liq. Cryst.*, 41, 861.
- [13] Cai, R., & Samulski, E. T. (1991). *Liq. Cryst.*, 9, 617.
- [14] Zhang, B. Y., Jia, Y. G., Yao, D. S., & Dong, X. W. (2004). *Liq. Cryst.*, 31, 339.
- [15] Colling, P. J., & Hird, M. (1998). *Introduction to Liquid Crystals: Chemistry and Physics*, Taylor & Francis: Bristol, U.K.
- [16] Eichhorn, S. H., Paraskos, A. J., Kishikawa, E., & Swager, T. M. (2002). *J. Am. Chem. Soc.*, 124, 12742.
- [17] Dimitrowa, K., Hauschild, J., Zashke, H., & Schubert, H. (1980). *J. Prakt. Chem.*, 331, 631.
- [18] Sung, H. H., & Lin, H. C. (2004). *Liq. Cryst.*, 31, 831.
- [19] Dingemans, T. J., & Samulski, E. T. (2000). *Liq. Cryst.*, 27, 131.
- [20] Mochizuki, H., Hasui, T., Tsutsumi, O., Kanazawa, A., Shiono, T., Ikeda, T., Adachi, C., Taniguchi, Y., & Shirota, Y. (2001). *Mol. Cryst. Liq. Cryst.*, 365, 129.
- [21] Haristoy, D., & Tsiourvas, D. (2003). *Chem. Mater.*, 15, 2079.
- [22] Lehmann, M., Kohn, C., Kresse, H., & Vakhovskaya, A. (2008). *Chem. Commun.*, 1768.
- [23] Lai, C., Ke, Y. C., Su, J. C., Shen, C., & Li, W. R. (2002). *Liq. Cryst.*, 29, 915.
- [24] Han, J., Zhang, F. Y., Wang, J. Y., Wang, Y. M., Pang, M. L., & Meng, J. B. (2009). *Liq. Cryst.*, 36, 825.
- [25] Han, J., Zhang, M., Wang, F., & Geng, Q. (2010). *Liq. Cryst.*, 37, 1471.
- [26] Zhu, L. R., Yao, F., Han, J., Pang, M. L., & Meng, J. B. (2009). *Liq. Cryst.*, 36, 209.
- [27] Wen, C. R., Wang, Y. J., Wang, H. C., Sheu, H. S., Lee, G. H., & Lai, C. K. (2005). *Chem. Mater.*, 17, 1646.
- [28] Cristiano, R., Vieira, A. A., Ely, F., & Gallardo, H. (2006). *Liq. Cryst.*, 33, 381.
- [29] He, C. F., Richards, G. J., Kelly, S. M., Contoret, A. E. A., & O'Neill, M. (2007). *Liq. Cryst.*, 34, 1249.
- [30] Qu, S., Chen, X., Shao, X., Li, F., Zhang, H., Wang, H., Zhang, P., Yu, Z., Wu, K., Wang, Y., & Li, M. (2008). *J. Mater. Chem.*, 18, 3954.
- [31] Yelamaggad, C. V., Achalkumar, A. S., Rao, D. S. S., & Prasad, S. K. (2009). *J. Org. Chem.*, 74, 3168.
- [32] Kang, S., Saito, Y., Watanabe, N., Tokita, M., Takanishi, Y., Takezoe, H., & Watanabe, J. (2006). *J. Phys. Chem. B*, 110, 5205.
- [33] Reddy, R. A., & Tschierske, C. (2006). *J. Mater. Chem.*, 16, 907.
- [34] Gortz, V., & Goodby, J. W. (2005). *Chem. Commun.*, 3262.
- [35] Gallardo, H., Ely, F., Bortoluzzi, A. J., & Conte, G. (2005). *Liq. Cryst.*, 32, 667.
- [36] Majumdar, K. C., Shyam, P. K., Rao, D. S. S., & Prasad, S. K. (2012). *Liq. Cryst.*, 39, 1358.
- [37] Belaissaoui, A., Cowling, S. J., & Goodby, J. W. (2013). *Liq. Cryst.*, 40, 421.
- [38] Wang, L., He, W., Wang, M., Wei, M., Sun, J., Chen, X., & Yang, H. (2013). *Liq. Cryst.*, 40, 354.
- [39] Yang, X., Dai, H., He, Q., Tang, J., Cheng, X., Prehm, M., & Tschierske, C. (2013). *Liq. Cryst.*, 40, 1028.
- [40] Frizon, T. E., Dal-Bo, A. G., Lopez, G., Silva Paula, M. M., & Silva, L. (2004). *Liq. Cryst.*, 41, 1162.
- [41] Nagaraj, M., Usami, K., Zhang, Z., Gortz, V., Goodby, J. W., & Gleeson, H. F. (2014). *Liq. Cryst.*, 41, 800.
- [42] Vieira, A. A., Caverio, E., Romero, P., Gallardo, H., Serrano, J. L., & Sierra, T. (2014). *J. Mater. Chem. C*, 2, 7029.
- [43] Han, J. (2013). *J. Mater. Chem. C*, 1, 7779.
- [44] Liao, Ch. T., Wang, Y. Ju., Huang, Ch. S., Sheu, H. S., Lee, G. H., & Lai, Ch. K. (2007). *Tetrahedron*, 63, 12437.

- [45] Hughes, G., & Bryce, M. R. (2005). *J. Mater Chem.*, 15, 94.
- [46] Tokohisa, H., Era, M., & Tsutsui, T. (1998). *Adv. Mater.*, 10, 404.
- [47] Qu, S., Lu, Q., Wu, S., Wang, L., & Liu, X. (2012). *J. Mater. Chem.*, 22, 24605.
- [48] Nijegorodov, N. I., & Downey, W. S. (1995). *Spectrochim. Acta. A.*, 51, 2335.
- [49] Shirota, Y., & Kageyama, H. (2007). *Chem. Rev.*, 107, 953.
- [50] Kulkarni, A. P., Tonzola, C. J., Babel, A., & Jenekhe, S. A. (2004). *Chem. Mater.*, 16, 4556.
- [51] Ahn, J. H., Wang, C., Pearson, C., Bryce, M. R., & Petty, M. C. (2004). *Appl. Phys. Lett.*, 85, 1283.
- [52] Li, X. C., Cacialli, F., Giles, M., Gruner, J., Friend, R. H., Holmes, A. B., Moratti, S. C., & Yong, T. M. (1995). *Adv. Mater.*, 7, 898.
- [53] Li, A. F., Ruan, Y. B., Jiang, Q. Q., He, W. B., & Jiang, Y. B. (2010). *Chem. Eur. J.*, 16, 5794.
- [54] Bhatia, S., & Gupta, M. (2011). *J. Chem. Pharm. Res.*, 3, 137.
- [55] Salimgareeva, V. N., Polevoi, R. M., Ponomareva, V. A., Sannikova, N. S., Kolesov, S. V., & Lep-lyanin, G. V. (2003). *J. Appl. Chem.*, 76, 1655.
- [56] Chudgar, N. K., Shah, S. N., & Vora, R. A. (1989). *Mol. Cryst. Liq. Cryst.*, 172, 51.
- [57] Mahadeva, J., Umesha, K. B., Rai, K. M. L., & Nagappa, N. (2009). *Mol. Cryst. Liq. Cryst.*, 509, 274.
- [58] (a) Parra, M., Fuentes, G., Vera, V., Villouta, Sh., & Hernandez, S. (1995). *Bol. Soc. Chil. Quim.*, 40, 455; (b) Parra, M., Belmar, J., Zunza, H., Zuniga, C., Fuentes, G., & Martinez, R. (1995). *J. Prakt. Chem.*, 337, 239; (c) Aguilera, C., Parra, M., & Fuentes, G. (1995). *Z. Naturforsch.*, 53B, 367.
- [59] (a) Parra, M., Hernandez, S., Alderete, J., & Zuniga, C. (2000). *Liq. Cryst.*, 27, 995; (b) Parra, M., Alderete, J., Zuniga, C., Hidalgo, P., Vergara, J., & Fuentes, G. (2002). *Liq. Cryst.*, 29, 1375; (c) Parra, M., Hidalgo, P., Carrasco, E., Barbera, J., & Silvino, L. (2006). *Liq. Cryst.*, 33, 875; (d) Parra, M., Hidalgo, P., & Elgueta, E. Y. (2008). *Liq. Cryst.*, 35, 823; (e) Parra, M., Hidalgo, P., Soto-Bustamante, E. A., Barbera, J., Elgueta, E. Y., & Trujillo-Rojo, V. H. (2008). *Liq. Cryst.*, 35, 1251; (f) Parra, M., Elgueta, E., Jimenez, V., & Hidalgo, P. (2009). *Liq. Cryst.*, 36, 301; (g) Barbera, J., Godoy, M. A., Hidalgo, P., Parra, M., Ulloa, J. A., & Vergara, J. M. (2011). *Liq. Cryst.*, 38, 679.
- [60] Hetzheim, A., Wesner, C., Werner, J., Kresse, H., & Tschierske, C. (1999). *Liq. Cryst.*, 26, 885.
- [61] Neises, B., & Steglich, W. (1978). *Angew. Chem. Int. Edit. Engl.*, 17, 522.
- [62] Li, X., Cui, J., Zhang, W., Huang, J., Li, W., Lin, C., Jiang, Y., Zhang, Y., & Li, G. (2011). *J. Mater. Chem.*, 21, 17953.
- [63] Subrahmanyam, S. V., Chalapathi, P. V., Mahabaleswara, S., Srinivasulu, M., & Potukuchi, D. M. (2014). *Liq. Cryst.*, 41, 1130.
- [64] Gray, G. W., (1979). In: *The Molecular Physics of Liquid Crystals*, Luckhurst, G. R. & Gray, G. W. (Eds.), Chaps. 1 & 12, Academic Press: New York.
- [65] Castellano, J. A., Goldmacher, J. E., Barton, L. A., & Kane, J. S. (1968). *J. Org. Chem.*, 33, 3501.